

広島大学学術情報リポジトリ
Hiroshima University Institutional Repository

Title	Intrusion Mechanism of a Granite Batholith
Author(s)	SAKURAI, Yasuhiro; YOSHIDA, Hironao; HARA, Ikuo
Citation	Journal of science of the Hiroshima University. Series C, Geology and mineralogy , 8 (2) : 103 - 122
Issue Date	1983-11-30
DOI	
Self DOI	10.15027/53101
URL	https://ir.lib.hiroshima-u.ac.jp/00053101
Right	
Relation	



Intrusion Mechanism of a Granite Batholith

By

**Yasuhiro SAKURAI, Hironao YOSHIDA
and Ikuo HARA**

with 16 Text-figures and 2 Plates

(Received May 30, 1983)

ABSTRACT: The Yagyū batholith, which is placed in the northern margin of the Ryōke belt of the Central Kinki Province, Japan, is one of granite batholiths which intruded after the regional metamorphism and strong regional-tectonism in the Ryōke belt ceased. The intrusion mechanism of the southern half of Yagyū batholith has been analysed in this paper. It is a zoned pluton, whose mantle and core consist mainly of quartz diorite — granodiorite facies and of adamellite facies respectively, and forms a tongue-like shape jutting toward the south. The gneissosity develops concordantly with the shape of the batholith and the intensity tends to increase from its core toward its margin. The structural trends of wall rocks are generally parallel or subparallel to the batholith boundary, showing that the southern half of Yagyū batholith had forcefully intruded forming gneissosity and strongly deforming its wall rocks.

Microtextures of constituent minerals (quartz and plagioclase) of the Yagyū batholith have been analysed. Quartz is recognized as two textural units, quartz grains and quartz pools: quartz grains as individual crystals distinguished from each other by high-angle boundaries, and quartz pools as individual domains occupied only or almost only by quartz grains and bounded mainly by other minerals than quartz. It has been clarified that quartz pools were commonly initially older single quartz grains as one of magmatic crystallization-induced microtextures and strongly elongated during the forceful intrusion of the batholith, and that quartz grains as constituents of quartz pools are secondary grains produced by dynamic recrystallization of older quartz grains related to the deformation which occurred after the emplacement of the batholith had been almost completely performed. Plagioclase also is recognized as two textural units, plagioclase grains and plagioclase pools: plagioclase grains as individual crystals distinguished from each other by distinct boundaries, and plagioclase pools as individual domains occupied only or almost only by plagioclase grains, showing euhedral outlines and single zonal structures of chemical composition. It has been pointed out that plagioclase grains (pl-grains) as constituents of plagioclase pools tend to increase in number but to decrease in size with increase of the intensity of development of gneissosity, showing that the formation of pl-grains is ascribed to the deformation related to the formation of gneissosity during the forceful intrusion of the batholith. The formation mechanism of pl-grains has been also briefly considered. And it has been concluded that, when the intrusion of the southern half of Yagyū batholith began, the lithofacies fractionation had already ceased and its mantle had already been almost completely consolidated.

CONTENTS

- I. Introduction
- II. Macroscopic structures of Yagyū granite batholith
 - A. Internal structures
 - B. Contact relationship between Yagyū batholith and its wall rocks
- III. Microtextures of constituent minerals
 - A. Quartz

- B. Plagioclase
 - 1. Distribution pattern of plagioclase
 - 2. Formation mechanism of pl-grains
 - a) Geometry of pl-grains
 - b) Material along neoboundaries
 - c) Formation of pl-grains
- References

I. INTRODUCTION

Late Mesozoic granites in Southwest Japan are distributed within a wide zone, whose southern margin is sharply bounded by the Median Tectonic Line, Ryoke belt and its northern non-metamorphic belt (Fig. 1). The major structure of this zone is mainly characterized by an echelon upright folds which were produced through the process of formation of Fossa Magna syntaxis under non-uniform compression from Pacific Ocean side (HARA and HIDE, 1974; HARA *et al.*, 1980a). The Late Mesozoic granites in Southwest Japan are divided into three groups in terms of time-relationship between their intrusion and the upright folding (HARA, 1979a and b; HARA *et al.*, 1980a; SEO *et al.*, 1981): 1) pre-upright folding granites which are of large-scale sheets in mode of occurrence and involved in large-scale upright folds together with their surrounding metamorphics, 2) syn-upright folding granites which occur as elongated bodies oriented parallel to the axial trends of upright folds, and 3) younger granites which had intruded after the upright folding. The granites of the former two groups are inclusively designated as older granites. They appear to be found only within the Ryoke belt. While the younger granites are developed throughout the Ryoke belt and its northern non-metamorphic belt. Most of Late Mesozoic granites in Southwest Japan belong to the group of the younger granites.

The younger granites have been considered to have intruded after the regional metamorphism and strong regional-tectonism in the Ryoke belt ceased. This is because they generally show no remarkable deformation structures. Therefore, they have been designated as post-tectonic granites. The fact that the younger granites had not undergone conspicuous deformation under regional tectonic stress field would be clearly convenient for analysis of modes of emplacement of their bodies. Our present concern in this paper is decipherment of intrusion mechanism of the Yagyu granite batholith, which is one of the typical batholiths of younger granites and placed in the northern margin of the Ryoke belt of the Central Kinki Province, Japan, (Fig. 1). The intrusion mechanism of the Yagyu batholith will be considered on the basis of analysis of its macroscopic structures (e.g. orientation patterns of lithofacies and gneissosity, and contact relation of it to its wall rocks) and microtextures of its constituent minerals.

The part of the Yagyu batholith, which is shown in Fig. 1, is surrounded by the Ryoke metamorphic rocks and older granites and not intruded by any younger granite, though it is partially covered by Cenozoic sediments in its eastern margin. The batholith is divided into two parts by a fault of ENE-WSW trend (Kizugawa fault), northern half and southern half of batholith. The intrusion mechanism of the southern half of batholith will be mainly analysed in this paper.

The field works for this study have been financially supported in part by the Grant in Aid for Scientific Researches from the Ministry of Education, Japan, (No. 57540480).

Intrusion Mechanism of a Granite Batholith

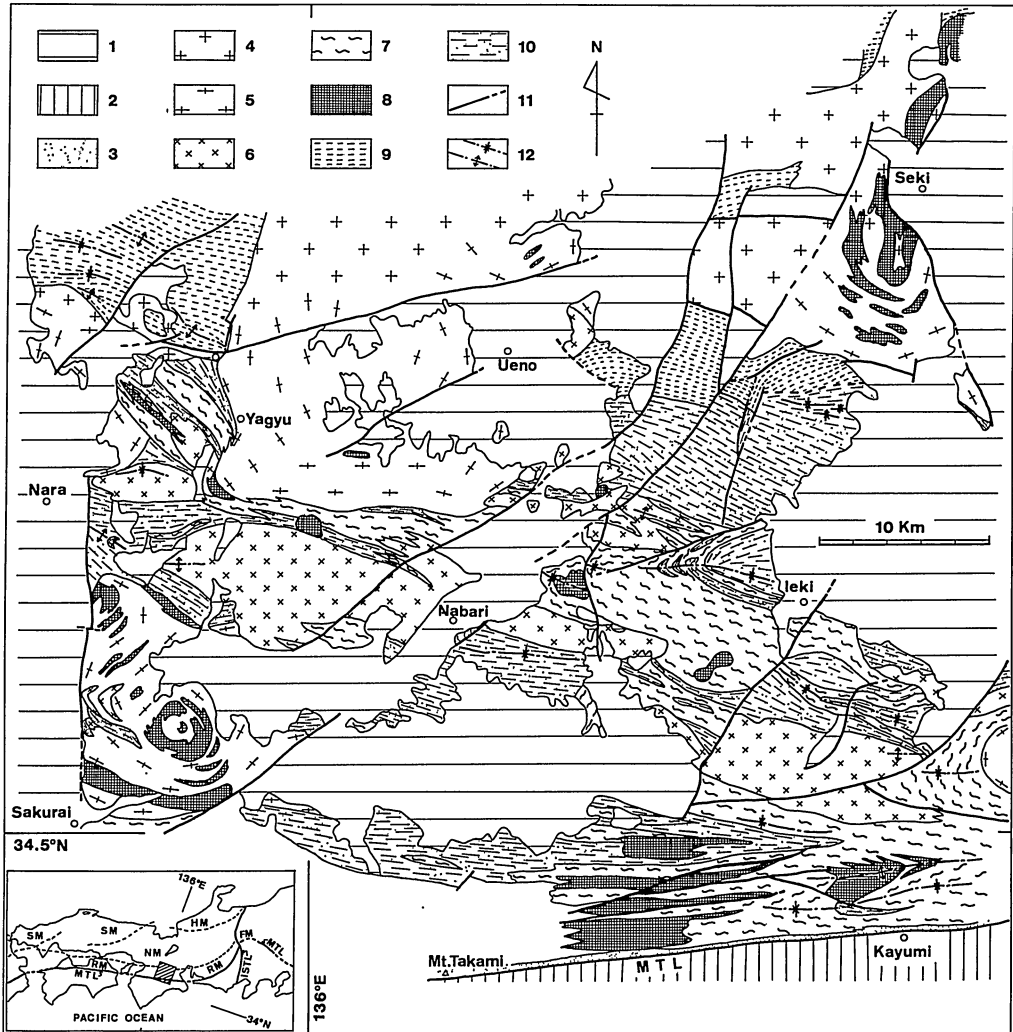


FIG. 1. The geological map of the Ryoke belt of the Central Kinki Province [compiled from the data of YOSHIZAWA *et al.* (1966) and ITO (1978)].

1: Cenozoic sediments, 2: Sambagawa schists, 3: strongly mylonitized rocks along Median Tectonic Line, 4 and 5: younger granites (4: massive type, 5: gneissose type), 6: syn-upright folding granites, 7: pre-upright folding granites, 8: metabasites, 9 and 10: Ryoke metamorphic rocks (9: schistose hornfels and slate, 10: gneisses), 11: fault, 12: axial traces of anticlines and synclines. MTL: Median Tectonic Line, ISTL: Itoigawa-Shizuoka Tectonic Line, FM: Fossa Maguna, RM: Ryoke Metamorphic Belt, NM: Non-metamorphic Belt, SM: Sangun Metamorphic Belt, HM: Hida Metamorphic Belt.

II. MACROSCOPIC STRUCTURES OF YAGYU GRANITE BATHOLITH

A. INTERNAL STRUCTURES

The lithofacies of the Yagyu batholith is classified into three facies, quartz diorite facies, granodiorite facies and adamellite facies, on the basis of modal analysis of constituent minerals (Fig. 2). The mineral assemblage is nearly constant throughout three facies and consist mainly of quartz, plagioclase, potassium feldspar, biotite and hornblende. Modal quartz is nearly constant throughout three facies, commonly being within a range from 25% to 40% in the modal quartz-plagioclase-potassium feldspar diagram (Fig. 2). On the other hand, there is an obvious tendency that, the higher the plagioclase/(quartz+potassium feldspar) ratio becomes, the higher the colour index becomes (Fig. 2). Fairly large volume of hornblende is commonly measured in quartz

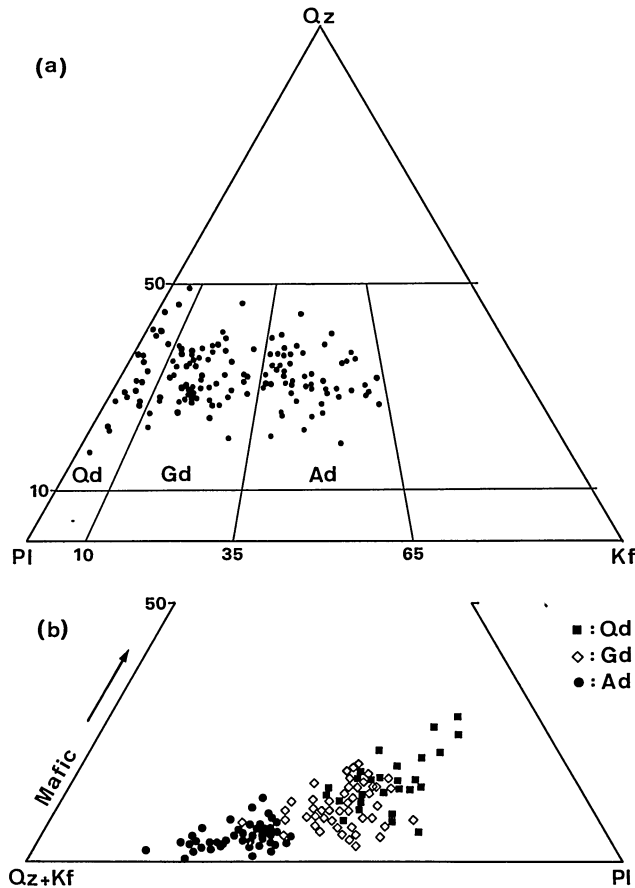


FIG. 2. Diagrams showing the results of modal analysis of main constituent minerals of Yagyu granite.

a: modal quartz—potassium feldspar—plagioclase diagram, b: modal mafic minerals—(quartz+potassium feldspar)—plagioclase diagram.

Qz: quartz, Kf: potassium feldspar, Pl: plagioclase, Mafic: mafic minerals, Qd: quartz diorite, Gd: granodiorite, Ad: adamellite.

The scheme of diagram (a) is after BATEMAN *et al.* (1963).

diorite facies, whereas it is only rarely found in adamellite facies.

Fig. 3 illustrates lithofacies distribution in the batholith which has been drawn on the basis of modal analysis of constituent minerals. Three facies distribute in separate zones or domains. In field observations, however, such lithofacies boundaries as shown in Fig. 3 can not be always detected as discontinuous planes. It can be pointed out that the

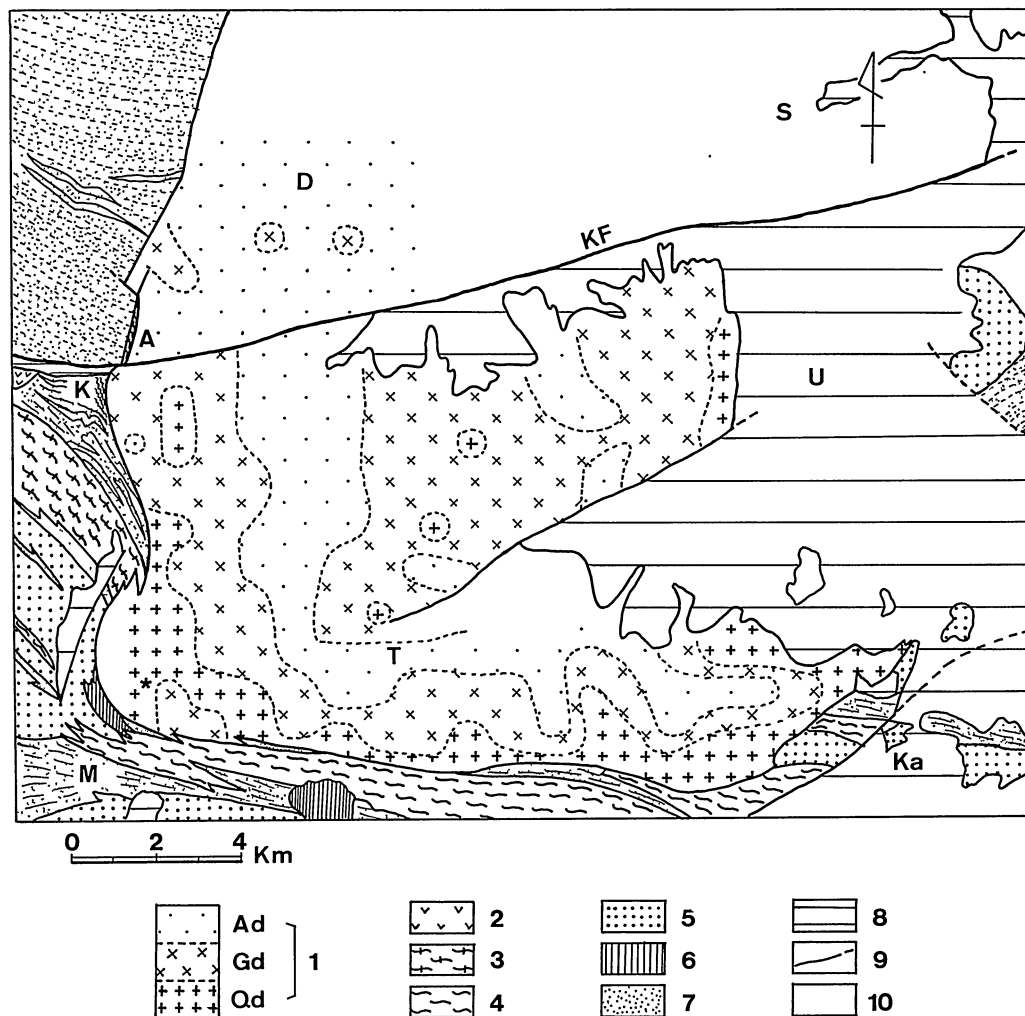


FIG. 3. The geological map of the Yagyū granite in which lithofacies distribution is partly shown.

1: Yagyū granite (Ad: adamellite facies, Gd: granodiorite facies, Qd: quartz diorite facies), 2 to 7: wall rocks of Yagyū granite [2: Koya granite (younger granite), 3: Sakawa granite (older granite), 4: Sugawa granodiorite (older granite), 5: fine-grained granites (older granite), 6: metabasites, 7: Ryoke metamorphic rocks], 8: Cenozoic sediments, 9: fault, 10: Yagyū granite (unclassified).

K: Kasagi, A: Ariichi, D: Dozenbo, S: Suwa, U: Ueno, M: Mima, T: Tsukigase, Ka: Iga-Kambe, KF: Kizugawa fault, * : locality of the specimen (Y-1-2) in which microtextures of plagioclase grains have been analysed in detail in this paper.

lithofacies gradually changes in most places.

The map of lithofacies distribution in the batholith (Fig. 3) shows that, in its southern half, there is a zonal arrangement of lithofacies: Quartz diorite facies, granodiorite facies and adamellite facies are successively exposed as zones from its margin toward its central part, granodiorite facies with quartz diorite facies being again widely distributed at the central part. Thus, it would be said that the southern half of batholith forms a kind of zoned pluton (cf. PITCHER, 1979). While, in the northern half of batholith, adamellite facies is widely exposed associating granodiorite facies in small areas.

Gneissosity, which is defined by parallel arrangement of mineral grains such as hornblende, biotite, feldspars and quartz, is recognized in the southern half and the southern margin of northern half of batholith (Fig. 4). The gneissosity surfaces in the margin of batholith are parallel or subparallel to the batholith boundary and generally steeply inclined. In the southern half of batholith their inclination angles show a distinct tendency to decrease toward its central part and they lie flat there (Fig. 4). Thus, it would be assumed that the overall arrangement of gneissosity surfaces forms a spoon-like shape

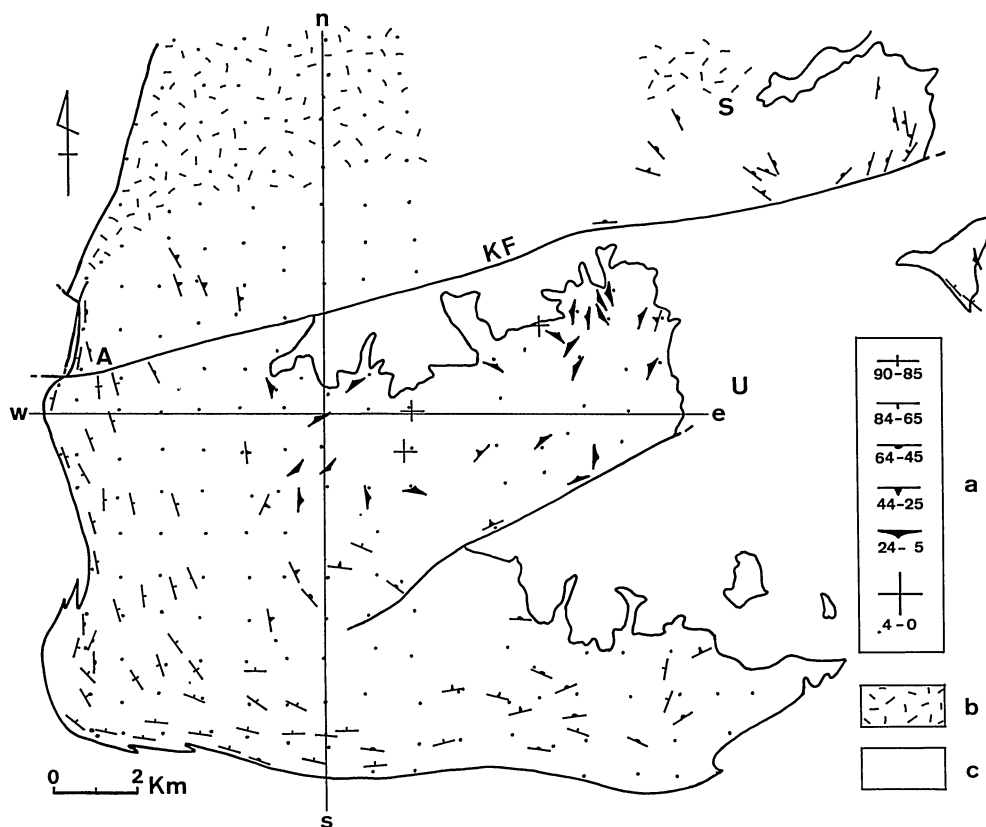


FIG. 4. Diagram showing the orientation pattern of gneissosity in Yagy granite.
 a: inclination angles of gneissosity, b: massive part, c: unclassified part,
 n-s and e-w: profile lines of Fig. 5, A: Ariichi, S: Suwa, U: Ueno,
 KF: Kizugawa fault.

Intrusion Mechanism of a Granite Batholith

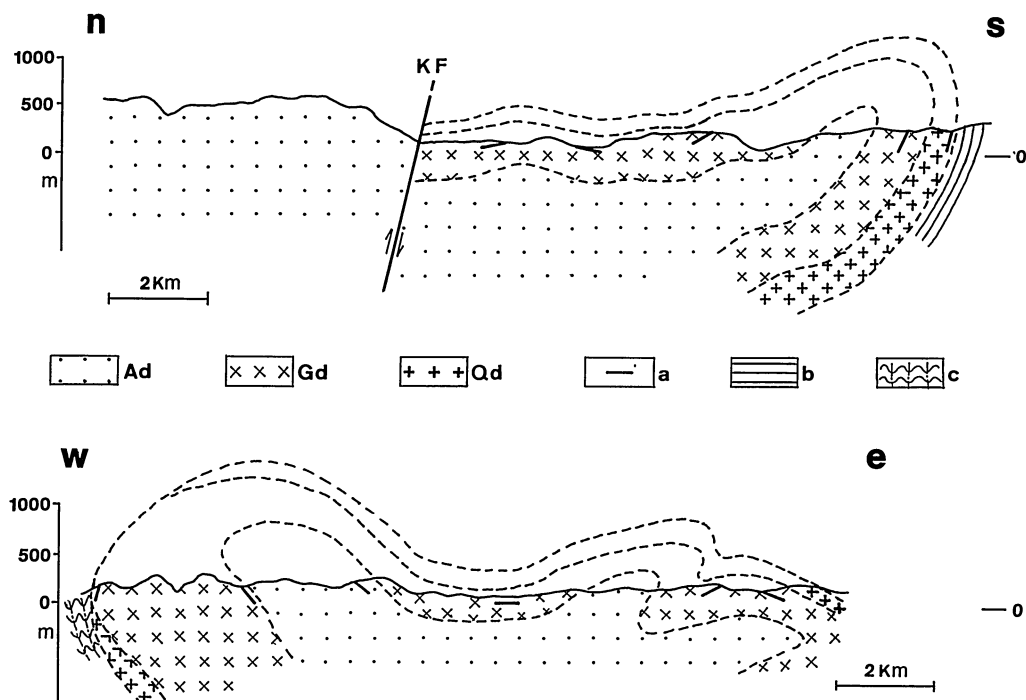


FIG. 5. The geological profiles of Yagyu granite along n-s and e-w lines in Fig. 4.

Ad: adamellite facies, Gd: granodiorite facies, Qd: quartz diorite facies, a: dip direction of gneissosity, b: gneisses (non-folded), c: gneisses (folded with axial plane cleavage), KF: Kizugawa fault.

for the southern half of batholith. The trends of gneissosity surfaces appear to be, as a whole, in harmony with those of the zonal arrangement of lithofacies (Fig. 3).

The intensity of development of gneissosity tends to decrease toward the north. In the southern margin of northern half of batholith gneissose granite appears to change gradually into massive one. In the southern half of batholith the intensity of development of gneissosity appears to change well dependently upon lithofacies: Generally, it is the weakest in adamellite facies, sometimes being even massive, and the strongest in quartz diorite facies. The gneissosity in adamellite facies of a small domain at the southwestern margin of batholith is strong, as well as that in its surrounding granodiorite facies. In the granodiorite facies of the central part of southern half of batholith the gneissosity is sometimes developed as strong as that in the quartz diorite facies of the southern margin of batholith.

In the southern half of batholith there is clearly a harmonic relationship between the mode of distribution of lithofacies and the pattern of development (orientation and intensity) of gneissosity. The orientation pattern of lithofacies and gneissosity is concordant with the batholith boundary (Figs. 3 and 4). On the basis of those evidences, thus, the three-dimensional shape and internal structure of the southern half of batholith would be drawn as shown in Fig. 5: The shape would be illustrated as a tongue-like one jutting toward the south, and the internal structure as a zoned pluton in which the

core consists of adamellite facies, the wall zone of granodiorite facies and the border zone mainly of quartz diorite facies.

B. CONTACT RELATIONSHIP BETWEEN YAGYU BATHOLITH AND ITS WALL ROCKS

The wall rocks of the Yagyu batholith consist of the Ryoke metamorphic rocks and older granites. The contact relationship between the batholith and its wall rocks is clearly observed in its western and southern margin (Fig. 1). The structural trends of wall rocks around the southern half of batholith are generally parallel or subparallel to the batholith boundary (Fig. 3) (HARA, 1962). Therefore, it can be said that the contact relationship is concordant and harmonic. While the structural trends of wall rocks around the northern half of batholith are generally approximately normal to the batholith boundary (Fig. 3), showing that the contact relationship is discordant and disharmonic (HARA, 1962).

Where the concordant-harmonic contact relationship is developed, the shistosity of metamorphic rocks adjacent to the batholith is parallel or subparallel in many places but highly oblique in some places to the batholith boundary. In the metamorphic rocks of the latter places are commonly developed minor folds with axial plane cleavage which is parallel or subparallel to the batholith boundary (Plate 10-1 and 2). In these photographs is also observed aplite vein folded together with surrounding metamorphic rocks. It is clear that the wall rocks were highly deformed by the intrusion of the batholith. The structural trends of the Ryoke metamorphic rocks and older granites in the Central Kinki Province are uniformly WNW-ESE (YOSHIZAWA *et al.*, 1966). However, they are locally rotated to NNW-SSE around the southern half of batholith (Fig. 1). Thus, it would be concluded that the southern half of batholith had forcefully intruded in a tongue-like shape (Fig. 5), forming gneissosity and strongly deforming its wall rocks.

In the northern half of batholith where the discordant-disharmonic contact relationship is developed, the shistosity of its adjacent metamorphic rocks is commonly oblique at high angles to the batholith boundary but not folded. And in them are frequently found granite veins or dykes, suggesting that the present batholith boundary and its surrounding narrow zone might have been a fracture zone immediately before the emplacement of the batholith occurred. The concordant-harmonic contact relationship is also quite locally observed along the fault of NNE-SSW trend in the southwestern margin of northern half of batholith (near Ariichi) (Fig. 3). From this evidence it would be assumed that in the lower horizon of the northern half of batholith a concordant-harmonic contact relationship develops though in its upper horizon a discordant-harmonic contact relationship does.

III. MICROTEXTURES OF CONSTITUENT MINERALS

A. QUARTZ

Quartz in the Yagyu batholith, as well as that in other younger and older granite batholiths in Southwest Japan, is recognized as two textural units as previously reported by the authors (SAKURAI and HARA, 1979; HARA *et al.*, 1980b): 1) quartz grains as individual crystals distinguished from each other by high-angle boundaries, and 2) quartz pools as individual domains occupied only or almost only by quartz grains and bounded

mainly by other minerals than quartz, although sometimes one quartz pool may be partly connected with the other. Here, the shapes of quartz pools in the Yagyu batholith will be analysed.

The shapes of quartz pools, as observed on thin sections, can be commonly approximated by ellipses (Plate 11-1 and 2). The longest axes of quartz pools are preferentially oriented parallel to the gneissosity where it is strongly developed (Plate 11-1), while they are randomly oriented where the granite is massive (Plate 11-2). Their orientation degree appears to increase with increase of the intensity of development of gneissosity.

The elongation degree ($E = \text{length of the longest axis} / \text{length of its normal}$) for 50 quartz pools in individual hand specimens have been measured on the thin sections normal to the gneissosity (the measurement for massive granite specimens has been done on the thin sections cut along the horizontal plane), and the average E -values have been obtained for individual specimens. Fig. 6 illustrates the spacial variation of the average E -value in the western part of the batholith. From this figure it can be pointed out that the average E -values smaller than 2.0 are commonly for quartz pools in massive granite while those in gneissose granite have the average E -values larger than 2.0. For quartz pools in strongly gneissose granite which develop in the southern margin and central part of the southern half of batholith, the average E -values are frequently larger than 2.5. The

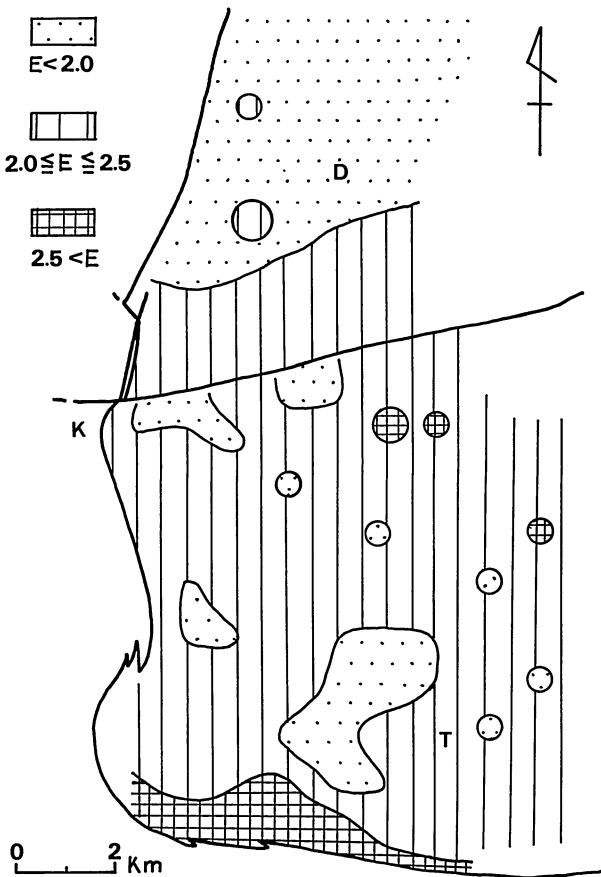


FIG. 6. Diagram showing variation of elongation degree (E) of quartz pools in Yagyu granite.

K: Kasagi, D: Dozenbo,
T: Tsukigase.

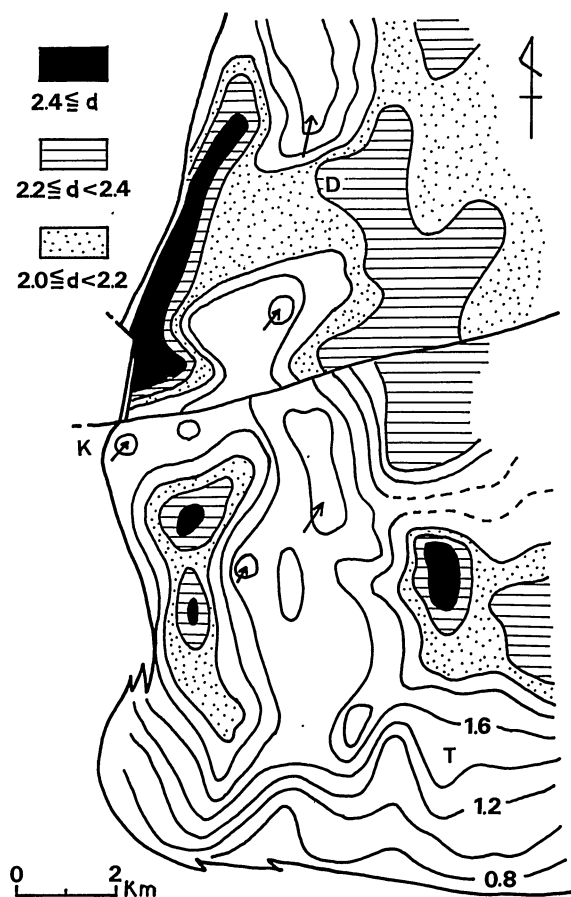


FIG. 7. Diagram showing the size distribution of quartz grains in Yagyu granite.

d: size in millimeter, K: Kasagi, D: Dozenbo, T: Tsukigase.

elongation degree of quartz pools appears to increase with increase of the intensity of development of gneissosity.

SAKURAI and HARA (1979) and HARA *et al.*, (1980b) have clarified that quartz grains (q-grains) as constituents of quartz pools are secondary grains produced by dynamic recrystallization of older quartz grains related to the deformation which occurred after the emplacement of the batholith had almost completely performed, and that quartz pools were initially occupied almost only by single older quartz grains and they were one of magmatic crystallization-induced microtextures. Fig. 7 illustrates the size distribution of q-grains in western part of the batholith. "The size of dynamically recrystallized grains does not significantly depend on temperature but depends only on the flow stress (LUTON and SELLARS, 1969; GLOVER and SELLARS, 1973)", as cited from NICOLAS and POIRIER (1976, p. 169). The pattern of size distribution of q-grains (Fig. 7) is not harmonic with that of spacial variation of the average E-values of quartz pools (Fig. 6). Thus, it is clear that the elongation of quartz pools is not related to the stress concentration in the batholith during the later stage of its cooling which formed q-grains. As mentioned in the preceding paragraph, the pattern of spacial variation of the average E-values of

Intrusion Mechanism of a Granite Batholith

quartz pools is harmonic with the mode of development of gneissosity. Thus, it would be assumed that quartz pools were elongated during the forceful emplacement of the batholith.

B. PLAGIOCLASE

1. Distribution pattern of plagioclase

Plagioclase in the Yagyu batholith is grasped on two textural units, 1) plagioclase grains as individual crystals distinguished from each other by distinct boundaries, and 2) plagioclase pools as individual domains occupied almost only by plagioclase grains, showing euhedral outlines and single zonal structures of chemical composition (Plate 11-3 and Figs. 8 and 9). Plagioclase pools consist either of some plagioclase grains or of single plagioclase grains. When plagioclase pools consist of some plagioclase grains, here, those grains as constituents of the plagioclase pools will be especially named pl-grains. It is clear that pl-grains are secondary grains produced by fragmentation of plagioclase pools (older single plagioclase grains), because the plagioclase pools show zonal structures of chemical composition.

In individual plagioclase pools, generally, extinction positions are slightly different between adjacent pl-grains and polysynthetic twin planes are displaced to some extent between them (Plate 11-3). Therefore, pl-grains are easily distinguished from each other. Contact ratio for pl-grains (PLG-PLG R) has been measured following ROGERS and BOGY's (1958) 'grain contact method'. Fig. 10 illustrates the spacial variation of

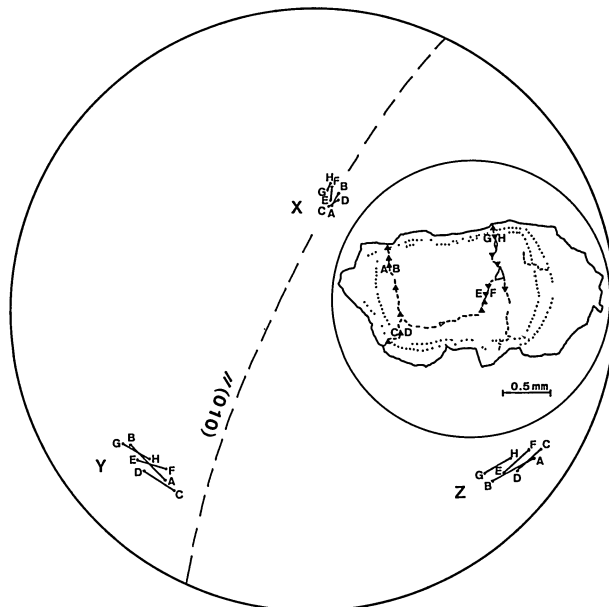


FIG. 8. Diagram showing the misorientation of lattice at the (010)-normal neo-boundaries in a plagioclase pool.

X: principal vibration axis X, Y: principal vibration axis Y, Z: principal vibration axis Z, A-B, C-D, E-F and G-H: positions in which lattice directions have been analysed.

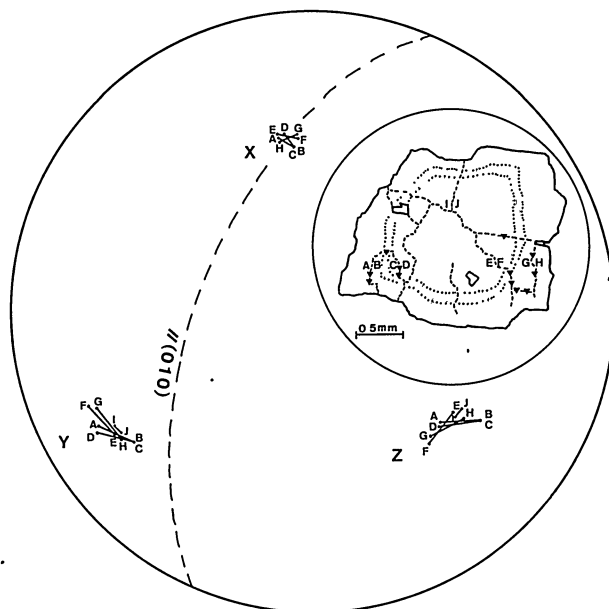


FIG. 9. Diagram showing the misorientation of lattice at the (010)-normal neo-boundaries in a plagioclase pool.

PLG-PLG R in the western part of batholith.

The high values of PLG-PLG R in the southern half of batholith are measured along its batholith boundary, the maximum value being 0.56 at the southwestern margin. Generally, PLG-PLG R is very low in the adamellite facies (Fig. 10). It is lower than 0.04 in the most part of the adamellite facies zone of the southern half of batholith. PLG-PLG R in the central part of the southern half of batholith shows the moderate values ranging from 0.05 to 0.24. PLG-PLG R higher than 0.05 are measured only where the gneissosity is recognizable, regardless of lithofacies. It tends to increase with increase of the intensity of development of gneissosity. Thus, it would be pointed out that PLG-PLG R is high in the mantle (=the wall and boarder zone) of the southern half of batholith and decreases toward its core.

Where PLG-PLG R is lower than 0.05, plagioclase pools consist only rarely of more than two pl-grains. While, where PLG-PLG R is larger than 0.25, they consist commonly of some pl-grains. Based on the definition of contact ratio (ROGERS and BOGY, 1958) and microscopic observation of plagioclase microtextures, it can be said that the higher values of PLG-PLG R means that plagioclase pools are composed of the greater number of pl-grains as measured on unit area and so of the smaller pl-grains in average size. Thus, from the distribution pattern of PLG-PLG R (Fig. 10), it would be assumed that the average size of pl-grains tends to decrease from the core toward the boarder zone of the southern half of batholith.

Where PLG-PLG R is higher than 0.25, such deformation microtextures as wavy extinction and bending of polysynthetic twin planes are commonly observed. While, where PLG-PLG is lower than 0.05, they are scarcely observed. The distribution pat-

Intrusion Mechanism of a Granite Batholith

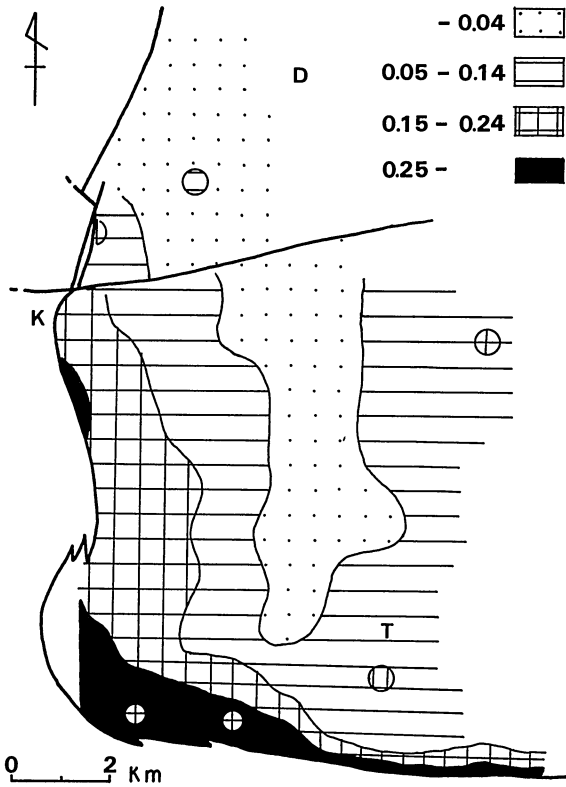


FIG. 10. Diagram showing the variation of contact ratio for pl-grains (PLG-PLG R) in Yagyu granite.

K: Kasagi, D: Dozenbo,
T: Tsukigase.

tern of PLG-PLG R (Fig. 10) is quite disharmonic with that of the size of q-grains (Fig. 7). As mentioned in the preceding paragraph, it is harmonic with the internal structure (gneissosity and lithofacies) of the southern half of batholith. Therefore, the formation of pl-grains would be ascribed to the deformation related to the formation of gneissosity during the forceful intrusion of the southern half of batholith.

2. Formation mechanism of pl-grains

The formation mechanism of pl-grains will be considered on the basis of analysis of microtextures of plagioclase in a hand specimen of quartz diorite (Y-1-2) which has been collected from the southern margin of the batholith (Fig. 3).

a) Geometry of pl-grains

The boundaries (neoboundaries) between pl-grains in individual plagioclase pools tend to be well developed nearly normal to polysynthetic albite twin plane, i.e. (010) (Plate 11-3). They appear to be also frequently parallel to (010). Generally, pl-grains appear to be mainly surrounded by neoboundaries of those two types, (010)-normal and (010)-parallel neoboundaries. The latter always appear connecting with the former. The zigzag shapes of neoboundaries (Plate 11-3 and Figs. 8 and 9) appear to be commonly related to the combined development of (010)-normal and (010)-parallel neoboundaries. The neoboundary directions are also apt to change around inclusion minerals.

The (010)-normal neoboundaries occupy 75% of the total length of neoboundaries which have been measured in 20 plagioclase pools. Therefore, they will be referred to as dominant component of neoboundaries, while the (010)-parallel neoboundaries as recessive component.

The difference in lattice orientation between pl-grains on both sides of neoboundary has been determined by the measurement of orientation direction of their principal vibration axes X, Y and Z. The angular scatters of Y axes at the (010)-normal neoboundaries are generally of the same magnitude as those of Z axes, being between 1.5° and 12°. The (010)-normal neoboundaries can be commonly referred to as high-angle boundaries. The angular scatters of X axes at the (010)-normal neoboundaries are less than 6°.

Figs. 8 and 9 illustrate the misorientation of lattice at the (010)-normal neoboundaries in two plagioclase pools. Both Y axes and Z axes scattering at the neoboundaries show a distinct tendency to be preferentially oriented on a great circle. The pole of the great circle, which corresponds to the average direction of the axes for rotation of Y axes and Z axes at the neoboundaries, coincides approximately with the center of distribution area of X-axes. The scattering of X axes at the (010)-normal neoboundaries, which occurs only in quite small angles, does not show any regular law.

The An content in portions of plagioclase pools, where the misorientation of lattice at the neoboundaries has been measured, is between 29 and 37 mol%. In plagioclase

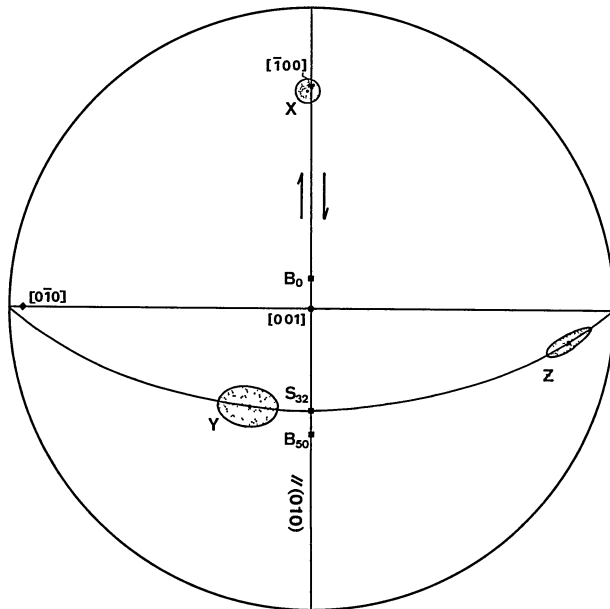


FIG. 11. Stereogram for gliding system on (010) in plagioclase (An_{80} - An_{35}) assumed from Figs. 9 and 10.

stippled areas: plots of distribution areas of X axes, Y axes and Z axes of Figs. 9 and 10, S_{32} : gliding direction, B_0 : gliding direction for plagioclase of An_0 , B_{50} : gliding direction for plagioclase of An_{50} [B_0 and B_{50} are cited from BORG and HEARD (1970)].

with such chemical composition, X axis is placed on or just near (010) and just near rhombic section (cf. Tsuboi *et al.*, 1977) (Fig. 11). According to the result of experimental deformation of plagioclase after BORG and HEARD (1970), both (010) and rhombic section are possible gliding planes. In plagioclase pools analysed in this section develops remarkably polysynthetic albite twin but only quite rarely pericline twin. In and around the portions of plagioclase pools, from which the data of Figs. 8 and 9 has been obtained, is also not commonly observed pericline twin but polysynthetic albite twin. Thus, it would be roughly pointed out that the formation of the (010)-normal neoboundaries is related to a kind of polygonization which was associated dominantly with gliding on (010). From the data of Figs. 8 and 9, the gliding direction on (010) would be assumed to coincide approximately with the intersecting line of (010) and plane containing Z axis and Y axis (S_{32} in Fig. 11).

Such gliding system on (010) appears to be harmonic with that experimentally predicted by BORG and HEARD (1970). However, what the random scattering of X axes at the (010)-normal neoboundaries means must be questioned.

While the angular scatters of principal vibration axes at the (010)-parallel neoboundaries are commonly less than 3° , showing that the misorientation of lattice at the neoboundaries may be quite small in magnitude. Therefore, it is difficult to understand the exact nature of the (010)-parallel neoboundaries only on the basis of optical observations.

b) *Material along neoboundaries*

From microprobe line traverses it has been clarified that along the neoboundaries frequently develop minute domains (N-spikes), in which abrupt decrease of An content occurs as shown in Fig. 12 as an example, and that their width is less than ca. $5 \mu\text{m}$. The

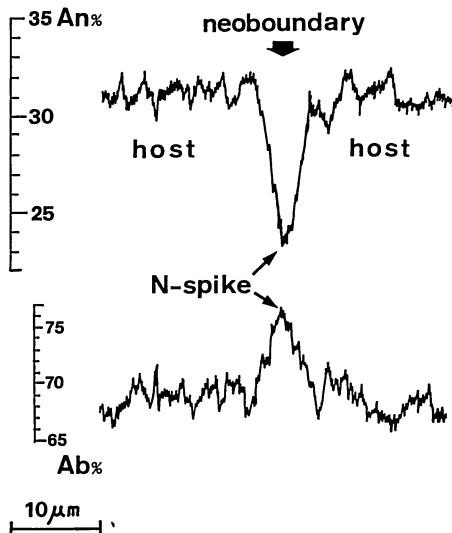


FIG. 12. Microprobe line traverses across a (010)-normal neoboundary in which the development of N-spike is recognized.

host plagioclase just adjacent to the N-spikes, which the authors have examined, has An-content of 29–37 mol%, though the plagioclase pools with pl-grains have zonal structures of compositional range shown in Fig. 13. Most of N-spikes are so narrow in width

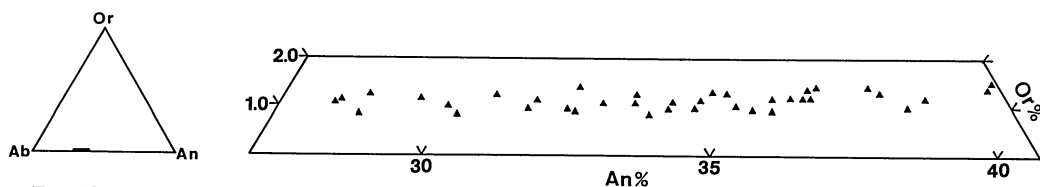


FIG. 13. Diagram showing the variation of chemical composition in pl-grains, except for N-spikes.

that their chemical composition can not be exactly determined by a JXA-5A microprobe with beam diameter of $2.5\ \mu\text{m}$ which is the most stable and easily obtainable minimum one. For N-spikes with width of larger than $3\ \mu\text{m}$, their chemical composition has been measured to be practically constant, regardless of that of their host: $\text{Ab}=74.9\text{--}76.1$, $\text{An}=24.5\text{--}23.5$ and $\text{Or}=0.6\text{--}0.4$, (Fig. 14). From microprobe line traverses it is judged that, for N-spikes with width of larger than $3\ \mu\text{m}$, the chemical variation at the boundaries between them and their host occurs commonly so suddenly that it can be regarded as to be discontinuous.

For the N-spikes with width of smaller than $3\ \mu\text{m}$ it is examined in Fig. 15 whether the chemical variation at the boundaries between them and their host occurs approximately discontinuously or not and whether their An content in minimum is constantly 24 mol% or not. Three numerical models of microprobe line traverses have been obtained on the basis of the following assumptions: 1) Measuring condition is such as beam diameter = $2.5\ \mu\text{m}$, sample driving speed = $10\ \mu\text{m}/\text{min}$ and time constant = 3, 2) Change in An content between N-spikes and their host is discontinuous, 3) An content within N-spikes is constant in 24 mol%, 4) An content of their host is 33 mol% for three models, and 5) their width is $1.5\ \mu\text{m}$, $2.0\ \mu\text{m}$ and $2.5\ \mu\text{m}$ for three models respectively. Data from the actual microprobe line traverses coincide almost completely with the numerical models. Thus it would be said for the N-spikes with width of less than $3\ \mu\text{m}$ that An content within them is constant in ca. 24 mol% and that the change in An-content between them and their host is discontinuous, like in the case of the N-spikes with width of larger than $3\ \mu\text{m}$.

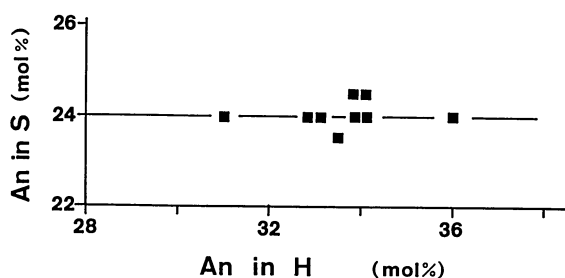


FIG. 14. Diagram showing the variation of An content in N-spikes which has been directly measured by JXA-5A microprobe.

An in S: An content in N-spike, An in H: An content in its host.

From the above-described evidences and considerations it could be assumed that the N-spikes are such domains of plagioclase as subgrains separated from their host. The An content (ca. 24 mol%) and Or content (ca. 0.5 mol%) of the N-spikes are clearly

lower than the minimum An content and Or content in the magmatic crystallization-induced zoning of plagioclase pools (Fig. 13). This fact means that the N-spikes (such domains as subgrains along the neoboundaries) had been formed under the lower temperature than the magmatic crystallization-induced zoning.

The widths of the N-spikes along the (010)-normal neoboundaries are between 1.5 μm and 5.5 μm , while they along the (010)-parallel neoboundaries are between 1.5 μm and 2.5 μm . As measured on the N-spikes along the (010)-normal neoboundaries, their widths show a distinct tendency to increase with increase of the misorientation of lattice at the neoboundaries (Fig. 16). Along the neoboundaries with the misorientation angles of less than 4° are only quite rarely detected N-spikes. The widths of the N-spikes

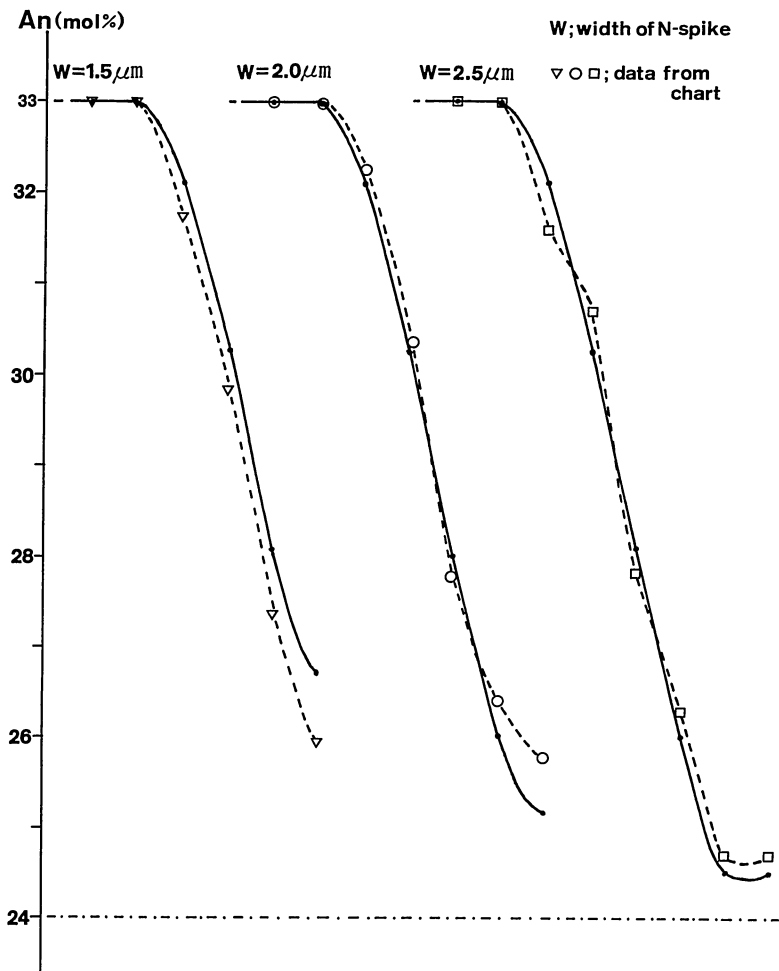


FIG. 15. Actual data (dashed lines) and numerical models (solid lines) of microprobe line traverses for N-spikes with width of smaller than 3 μm in which An content can not be directly measured by JXA-5A microprobe and whose host has commonly An content of 33%. For fuller explanation see Text.

appear to be independent of the An content in host and to increase stepwise with increase of the misorientation angles at the neoboundaries as shown by a line in Fig. 16. From this evidence it would be assumed that the N-spikes had intermittently grown releasing the high strain concentration in the vicinity of the neoboundaries which was induced by the progressive misorientation of pl-grains, i.e. there were induction intervals in the process of the growth of N-spikes during continued straining.

c) Formation of pl-grains

On the basis of the above-described evidences and considerations, the formation of pl-grains will be explained as follows. They firstly appeared as subgrains with primary (magmatic crystallization-induced) chemical composition, whose formation is ascribed to re-arrangement and elimination of dislocations produced dominantly by gliding on (010), i.e. to the dynamic recovery (cf. WHITE, 1977). The subgrains were progressively

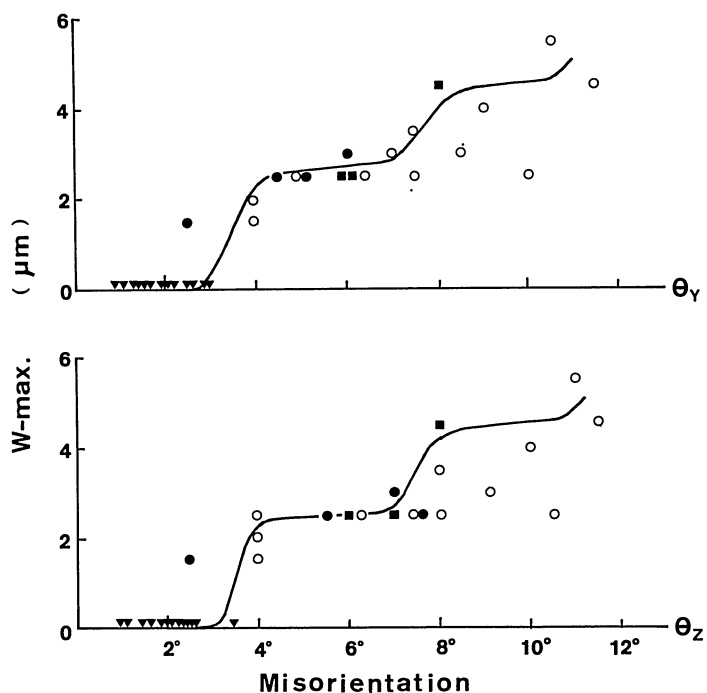


FIG. 16. Diagram showing relationship between the width of N-spike and the misorientation angle at the (010)-normal neoboundaries.

W-max.: maximum width of N-spike along individual neoboundaries, θ_Y : misorientation angle for Y axis at the position in which the maximum width of N-spike has been measured, θ_Z : misorientation angle for Z axis at the position in which the maximum width of N-spike has been measured, triangles: θ_Y and θ_Z at neoboundaries without N-spike, solid circles: data from N-spikes whose host has An content of 35.5–38.0%, open circles: data from N-spikes whose host has An content of 32.5–35.0%, solid squares: data from N-spikes whose host has An content of 29.5–32.0%.

rotated in the process of continued dynamic recovery as the bulk strain of the Yagyu granite increased, and became to be recognizable as pl-grains. Thus, the formation of pl-grains is referred to as the in situ dynamic recrystallization (cf. NICOLAS and POIRIER, 1976). The misorientation between adjacent pl-grains continuously increased with successive increase of the bulk strain of the granite. The progressive increase of misorientation caused high strain concentration near the neoboundaries between pl-grains. The stored strain energy was responsible for the nucleation and initial growth of the N-spikes, which are comparable with the nucleation and growth type of dynamic recrystallization (POIRIER and NICOLAS, 1975). The critical strain for the onset of the recrystallization appears to have been attained when the misorientation angles reached ca. 3–4° (Fig. 16) (see also LUTON and SELLARS, 1969). After the stored strain energy near the neoboundaries was released by the nucleation and initial growth of the N-spikes, their further growth must not have occurred until the strain energy was again sufficiently stored near the neoboundaries due to the progressive misorientation of pl-grains. When the critical strain near the neoboundaries was attained again, namely, the second cycle of the growth of N-spikes occurred. Such process was repeated during the progressive misorientation of pl-grains, giving rise to the relationship (Fig. 16) that the widths of the N-spikes increase stepwise with increase of the misorientation angles.

PLG–PLG R is high in the mantle of the southern half of Yagyu batholith, showing that plagioclase pools consist commonly of some pl-grains. From the above-described nature of pl-grains this fact is considered to mean that the granitic rocks (mainly quartz diorite facies and granodiorite facies) of the mantle had already been almost completely consolidated during the intrusion of the southern half of batholith. Thus, it can be said that the lithofacies zoning had already been produced before the beginning of its intrusion.

REFERENCES

- BATEMAN, P. C., CLARK, L. D., HURBER, N. K., MOORE, J. C., and RINHERT, C. D., (1963): The Sierra Nevada batholith — a synthesis of recent work across the central part. *U. S. Geol. Surv. Prof. pap.*, 414D, D1–D46.
- BORG, I. Y. and HEARD, H. C., (1970): Experimental deformation of plagioclase. In P. PAULITSCH, Ed., *Experimental and natural rock deformation*, p375–403. Springer, Berlin.
- GLOVER, G. and SELLARS, C. M., (1973): Recovery and recrystallization during high-temperature deformation of α -iron. *Metall. Trans.*, 4, 765–775.
- HARA, I., (1962): Studies on the structure of the Ryoke metamorphic rocks of the Kasagi district, Southwest Japan. *Jour. Sci. Hiroshima Univ.*, Ser. C, 4, 163–224.
- , (1979a): Analysis of movement picture of Late Mesozoic Tectonism in Honshu geosynclinal terrain of Southwest Japan. *Studies on Late Mesozoic tectonism in Japan*, 1, 1–4.
- , (1979b): Structural relationship between the Sambagawa and the Ryoke belt. *86th Annu. Meet. Geol. Soc. Japan (Abstract)*.
- HARA, I. and HIDE K., (1974): The origin of the Median Tectonic Line. *Marine Sci.*, 6, 34–40.
- HARA, I., SHOJI, K., SAKURAI, Y., YOKOYAMA, S. and HIDE, K., (1980a): Origin of the Median Tectonic Line and its initial shape. *Mem. Geol. Soc. Japan*, 18, 27–49.
- HARA, I., SAKURAI, Y., ARITA, M. and PAULITSCH, P., (1980b): Distribution pattern of quartz in granites — evidence of their high-temperature deformation during cooling. *N. Jb. Miner. Mh.*, H1, 20–30.
- ITO, M., (1978): Mylonitization of granitic rocks of the Kayumi district, Mie prefecture. *Median tectonic line*, 3, 99–101.

- LUTON, M. J. and SELLARS, C. M., (1969): Dynamic recrystallization in nickel-iron alloys during high-temperature deformation. *Acta Met.*, 17, 1033-1043.
- NICOLAS, A. and POIRIER, J. P., (1976): *Crystalline plasticity and solid state flow in metamorphic rocks*. John Wiley and Sons, Inc., New York.
- PITCHER, W. S., (1979): The nature, ascent and emplacement of granitic magmas. *J. Geol. Soc. London*, 136, 627-662.
- POIRIER, J. P. and NICOLAS, A., (1975): Deformation-induced recrystallization due to progressive misorientation of subgrains, with special reference to mantle peridotites. *J. Geol.*, 83, 707-720.
- ROGERS, J. J. and BOGY, D. B., (1958): A study of grain contacts in granite rocks. *Science*, 127, 470-471.
- SAKURAI, Y. and HARA, I., (1979): Studies on microfabrics of granites, with special reference to quartz fabric. *Mem. Geol. Soc. Japan*, 17, 287-294.
- SEO, T., YOKOYAMA, S. and HARA, I., (1981): Metamorphism and tectonism in the Ryoke metamorphic belt. In HARA, I. Ed., *Tectonics of paired metamorphic belts*, 65-72.
- TSUBOI, S., MIZUTANI, S., SUWA, K. and TSUZUKI, Y., (1977): *Charts of plagioclase optics*. Iwanami Shoten Publ., Tokyo.
- WHITE, S., (1977): Geological significance of recovery and recrystallization processes in quartz. *Tectonophysics*, 39, 143-170.
- YOSHIZAWA, H., NAKAJIMA, W. and ISHIZAKA, K., (1966): Accomplishment of a regional geological map. *Mem. Coll. Sci. Univ. Kyoto, Ser. B*, 22, 437-454.

Yasuhiro SAKURAI, Hironao YOSHIDA and Ikuo HARA:
INSTITUTE OF GEOLOGY AND MINERALOGY,
FACULTY OF SCIENCE, HIROSHIMA UNIVERSITY.

EXPLANATION OF PLATE X

- 1 and 2: Photographs of strongly folded metamorphic rocks along the boundary of the Yagyu batholith at Ariichi. The axial plane cleavage develops subparallel to the batholith boundary. Gr: Yagyu granite, Ap: aplite veins.

EXPLANATION OF PLATE XI

- 1: Photograph of gneissose part of Yagyu granite. Q: quartz pools.
- 2: Photograph of massive part of Yagyu granite. Q: quartz pools.
- 3: Microphotograph of plagioclase in Yagyu granite showing development of pl-grains. Plagioclase pool placed in the center of this microphotograph is shown in Fig. 8. Solid line, broken line and dotted line stand for pool boundary, neoboundary and boundary of chemical zoning, respectively.

